Science Advances
AAAS

Supplementary Materials for

Internally generated population activity in cortical networks hinders information transmission

Chengcheng Huang *et al*.

Corresponding author: Chengcheng Huang, huangc@pitt.edu

Sci. Adv. **8**, eabg5244 (2022)
DOI: 10.1126/sciadv.abg5244

The PDF file includes:

Other Supplementary Material for this manuscript includes the following:

Supplemental Information

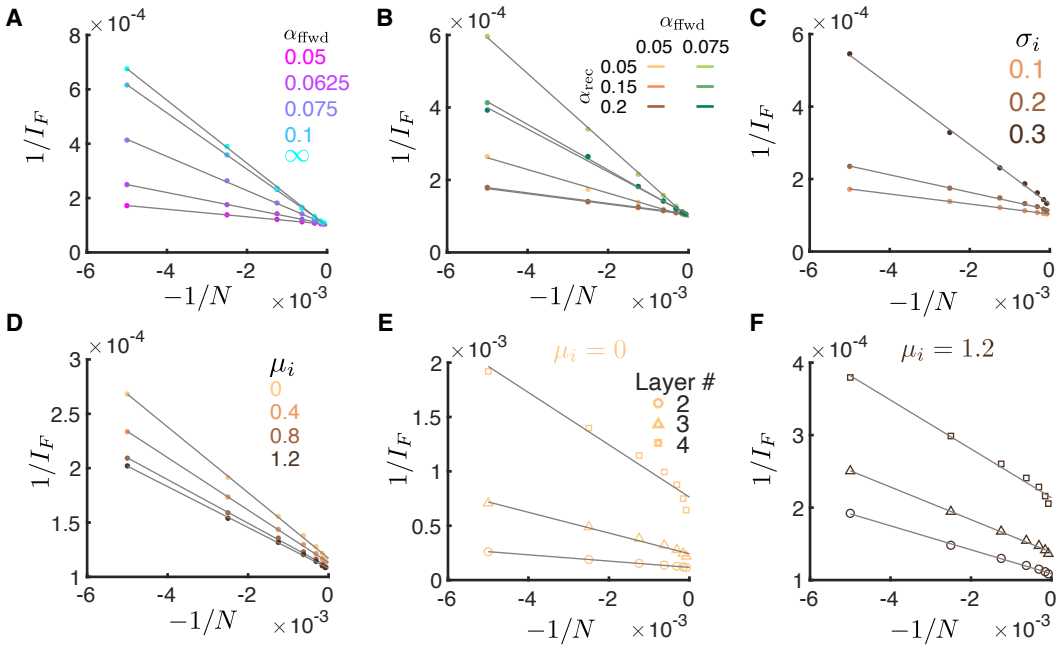

Figure S1: **Related to Figures 3, 4, 6, 8 and 9.** Summary of the linear fit of the inverse of the linear Fisher information ($1/I_F$) vs the inverse of the number of neurons ($1/N$) for estimating $1/I_F$ at the limit of $N \to \infty$ (Eq. 9, see Methods). **A**, Linear fit for networks of different feedforward projection widths (α_{ffwd}). Same I_F as shown in Fig. 3A. **B**, Linear fit for networks of different feedforward (α_{ffwd}) and recurrent(α_{rec}) projection widths. Same I_F as shown in Fig. 4A. **C**, Linear fit for networks of different inhibitory projection widths (σ_i). Same I_F as shown in Fig. 6A. **D**, Linear fit for networks with different depolarization current to the inhibitory neurons (μ_i). Same I_F as shown in Fig. 8A. **E,F**, Linear fit for multi-layer networks without input to the inhibitory neurons (E, $\mu_i = 0$) or with (F, $\mu_i = 1.2$). Same I_F as shown in Fig. 9B,C.

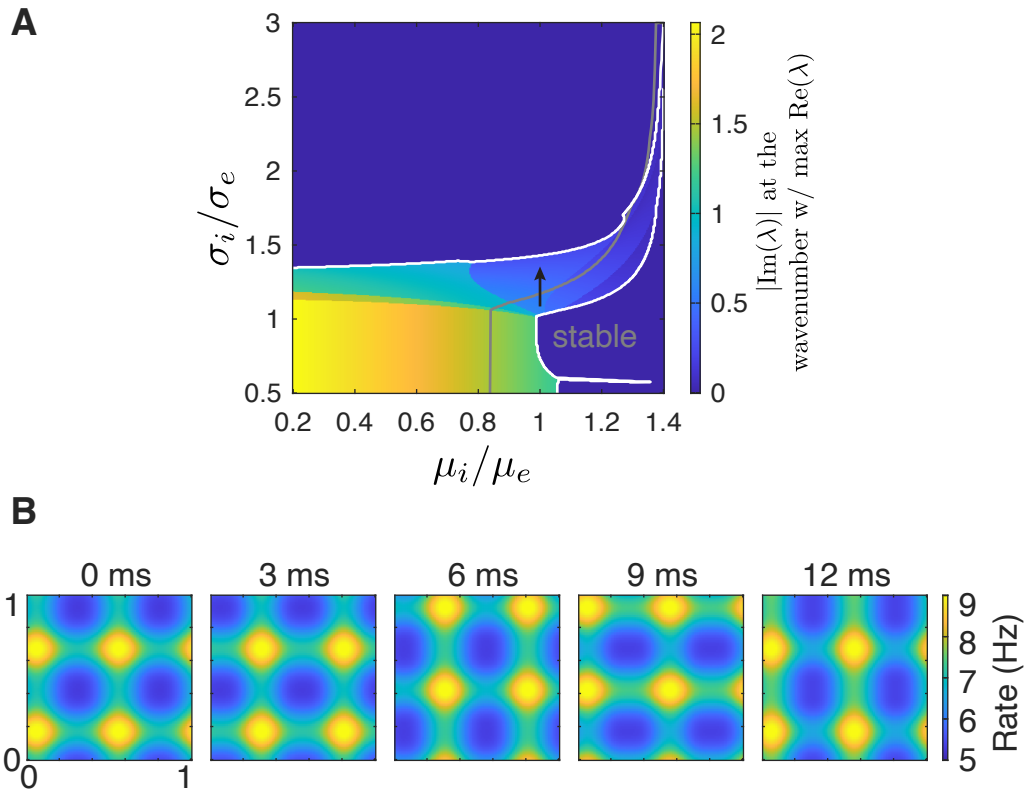

Figure S2: **Related to Figure 5.** A, Imaginary part of eigenvalues at the wavenumber that has the maximum real part of the firing rate model as a function of σ_i/σ_e and μ_i/μ_e. White curves are the contour of regions where the imaginary parts are zero. Gray curve is the boundary of the stable region (the gray region in Fig. 5A in main text). B, An example solution of the firing rate model just beyond the Turing-Hopf bifurcation during one period (black arrow in panel A, $\mu_i/\mu_e = 1, \sigma_i/\sigma_e = 1.175$).

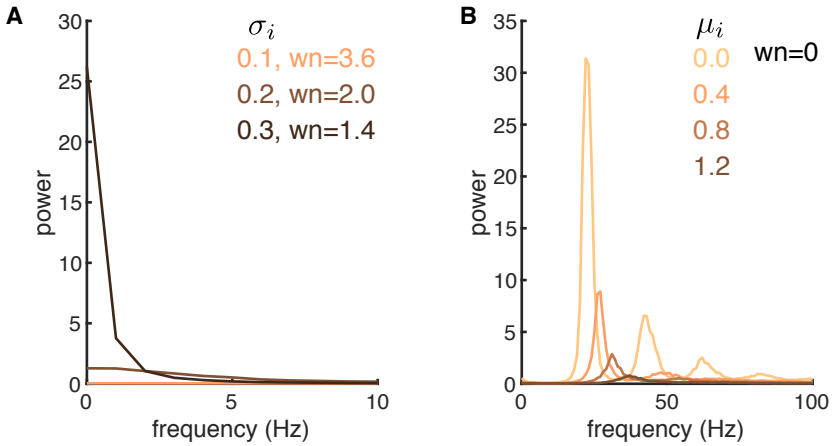

Figure S3: **Related to Figures 5 and 7.** Temporal spectra of spiking activity at the dominant wave number. A, Networks with different σ_i, related to Fig. 5. The wave numbers shown for networks with $\sigma_i = 0.1, 0.2, 0.3$ are 3.6, 2 and 1.4, respectively. B, Networks with different μ_i, related to Fig. 7. Temporal spectra at the zero wave number are shown. The temporal spectra were computed using 1 second time window.

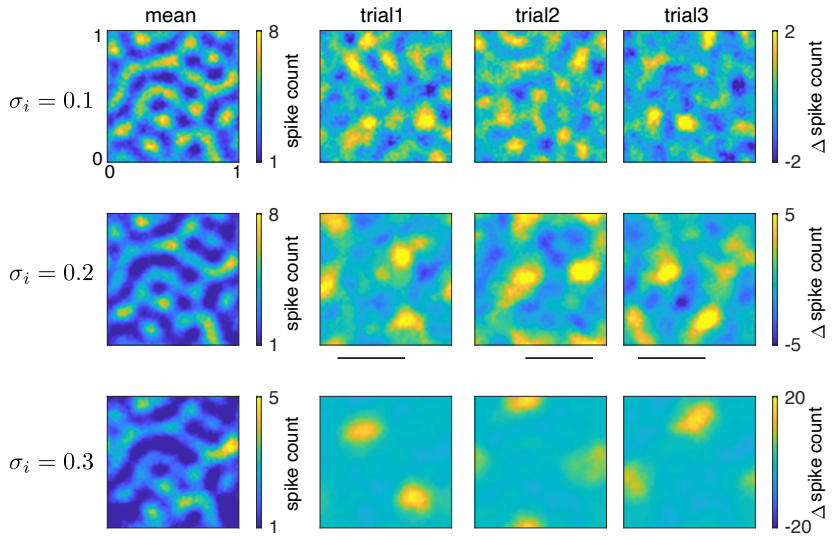

Figure S4: **Related to Figure 5.** The deviations of spike counts from the mean show spatial patterns of the internal dynamics in networks with different σ_i when driven by a Gabor image. Left, mean spike counts with 200 ms window. Right, three trials of mean (across trials) corrected spike counts from the network. Spike count examples are the same as shown in Fig. 5D. In the network with $\sigma_i = 0.2$, the wavenumber with the maximum real part of eigenvalues is 2 (Fig. 5A), which corresponds to a wavelength of 0.5. The deviations of spike counts show patterns with wavelength 0.5 in one spatial direction and wavelength 1 in the other direction (middle panel). In the network with $\sigma_i = 0.3$, the wavenumber with the maximum real part of eigenvalues is $\sqrt{2}$ (Fig. 5A), which corresponds to wavelength 1 in both x and y directions. The deviations of spike counts show patterns with wavelength 1 in both directions (bottom panel). The scale bar indicates a length of 0.5 (normalized unit). The spatial domain of the network is $[0, 1] \times [0, 1]$. Images are smoothed with a Gaussian kernel of width 0.01.

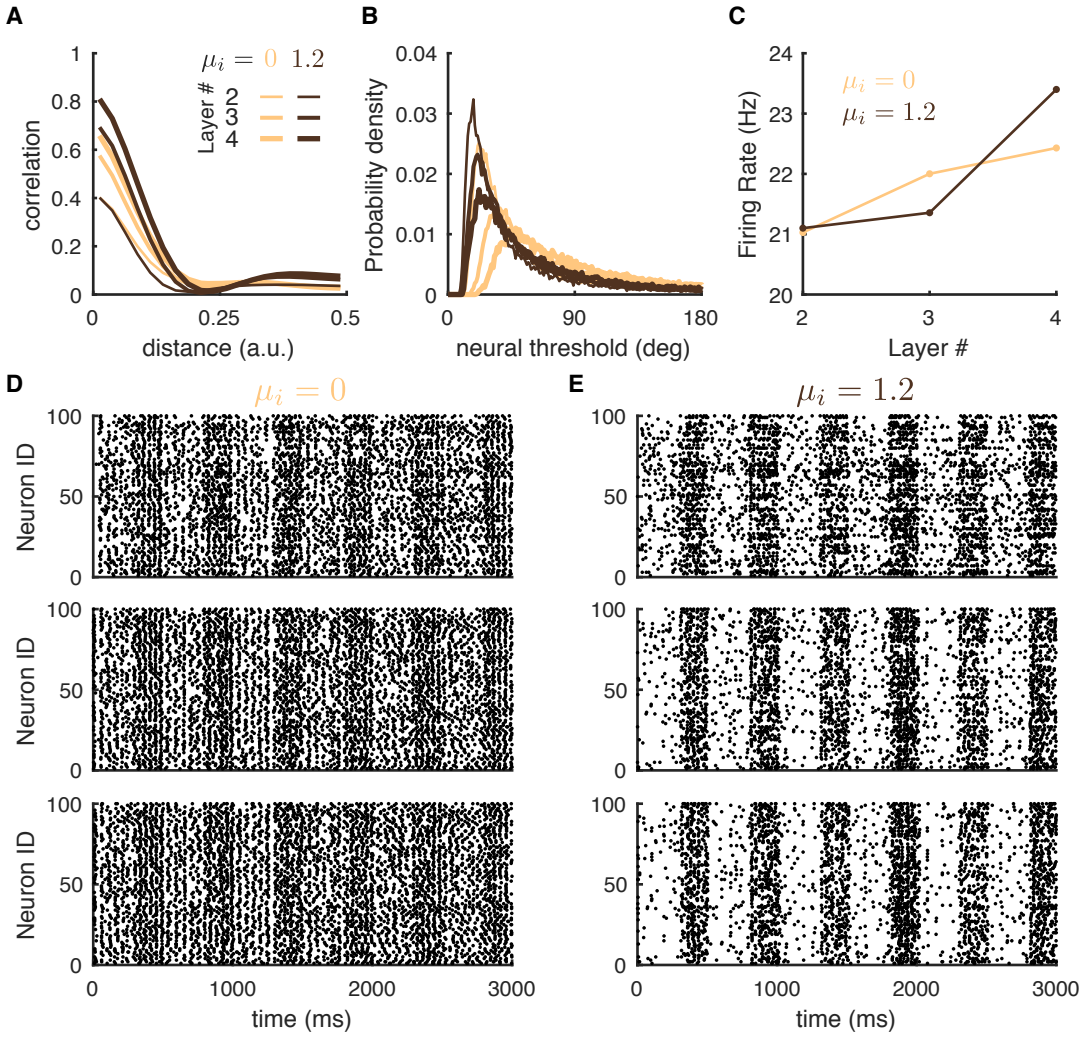

Figure S5: **Related to Figure 9.** The network responses in a multi-layer model with (orangel, $\mu_i = 0$) or without (dark brown, $\mu_i = 1.2$) depolarizing currents to the inhibitory neurons (μ_i) across layers. **A**, Pairwise correlations as a function of the distance between excitatory neuron pairs across layers (Layer 2, thin lines; Layer 3; medium-width lines; Layer 4; thick lines). **B**, The probability density distributions of neural thresholds (σ_i/f_i') of excitatory neurons across layers and in the two conditions of μ_i. **C**, The mean fring rates of the excitatory populations across layers. The feedforward strengths between layers were chosen such that the mean firing rates of layer 2-4 were similar across layers as well as between the two conditions of μ_i. **D**, The raster plots of 100 excitatory neurons randomly selected from Layer 2 to Layer 4 (top to bottom panel) in a network without depolarizing current to the inhibitory neurons ($\mu_i = 0$). The image was presented for 200 ms and then off for 300 ms in each trial. The average rates of Layer 1 neurons were 10 Hz during image presentation and 5 Hz when image was off. **E**, Same as **D** for a network with $\mu_i = 1.2$. The inputs from Layer 1 are the same in both conditions of μ_i. See Methods for model details.

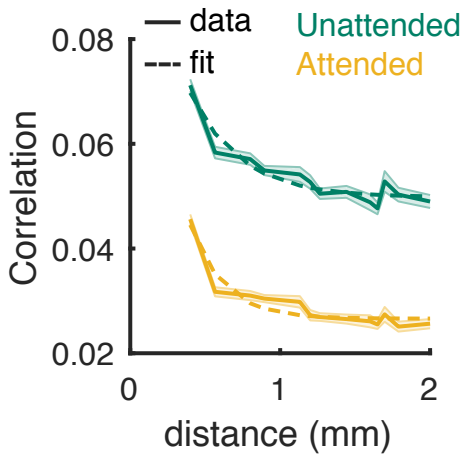

Figure S6: Spike count correlation as a function of distance from multi-electrode recordings in V4 area during a spatial attention task (data from Cohen and Maunsell (2009)). The decay rate λ_s was estimated to be $\lambda_s = 0.33$ mm (95% confidence interval (0.2461, 0.4193)) for the unattended state and $\lambda_s = 0.22$ mm (95% confidence interval (0.1721, 0.272)) for the attended state estimated by fitting an exponential function, $a + b \exp(-x/\lambda_s)$.

Supplementary Movie 1: Spiking activities of a spatially ordered network with $\sigma_i = 0.1$ and $\sigma_e = 0.1$, related to Figure 5. Each black dot indicates that the neuron at spatial position (x; y) fired within two milliseconds of the time stamp shown on top.

Supplementary Movie 2: Same as Movie 1 for a network with $\sigma_i = 0.2$ and $\sigma_e = 0.1$, related to Figure 5.

Supplementary Movie 3: Same as Movie 1 for a network with $\sigma_i = 0.3$ and $\sigma_e = 0.1$, related to Figure 5.

Supplementary Movie 4: Same as Movie 1 for a network with $\mu_i = 0$, related to Figure 7.

Supplementary Movie 5: Same as Movie 1 for a network with $\mu_i = 1.2$, related to Figure 7.